Solid Freeform Fabrication 2019: Proceedings of the 30th Annual International
Solid Freeform Fabrication Symposium – An Additive Manufacturing Conference
Reviewed Paper

Tailoring Physical Properties of Shape Memory Polymers for FDM-type Additive Manufacturing

Paulina A. Quiñonez [1,2] , Diego Bermudez [1,2], Leticia Ugarte-Sanchez [1,2] and David A. Roberson [1,2,*]

1. Polymer Extrusion Lab, The University of Texas at El Paso, El Paso TX, 79968
2. Department of Metallurgical, Materials and Biomedical Engineering, The University of Texas at El Paso, El Paso, TX 79968

* Corresponding Author: droberson@utep.edu

Abstract

Inclusion of shape memory polymers into additive manufacturing technologies based on fused deposition modeling (FDM™) can greatly increase the usefulness of this fabrication platform. Materials compatible with FDM™ such as polylactic acid (PLA) are known to exhibit shape memory properties, however aspects such as shape recovery and shape fixation are not tunable. The work presented here entails the initial development and characterization of shape memory polymers intended for FDM™-type additive manufacturing platforms. Here, two polymers with differing shape memory mechanisms (dual component and dual state) were combined in iterative ratios leading to material systems with tunable physical properties. Dynamic mechanical analysis (DMA) was used to determine the critical thermal parameters while polymer crystallinity was determined via x-ray diffraction (XRD). Scanning electron microscopy (SEM) was used to characterize the fracture morphology of impact test specimen.

Introduction

Advancing the applicability of manufacturing (AM) depends largely on the availability of materials with a wide range of physical properties as well as compatibility with a given AM platform. Particular to AM machines based on fused deposition modeling (FDM™) technology, two strategies are generally employed: 1) the creation of new polymer blends; and 2) the creation of new polymer matrix composites (Roberson, Shemelya, et al., 2015). A third strategy can also be utilized—exploring whether or not a polymer used in another application and processing scheme can be used in FDM™-type manufacturing—as was the case with NinjaFlex® a thermoplastic urethane (TPU) that was originally developed by Fenner Drives, Inc. to serve as belts in automated teller machines (ATM)s.

The premise of developing new materials for FDM™-type AM platforms becomes more profound if a system with tunable properties is developed. An example of a thermoplastic composite system with tunable X-ray shielding capability was demonstrated by Shemelya et al. (Shemelya et al., 2015) where the shield capability of polycarbonate was manipulated by varying the content of tungsten within the composite. Here the material system was compatible with desktop-grade fused filament fabrication (FFF) 3D printers and the intended application was to protect electronic systems in CubeSat satellite systems. An example of a FFF-compatible polymer blend system was made by Siqueiros et al. (Siqueiros et al., 2016) who demonstrated the development and characterization of rubberized acrylonitrile butadiene styrene (ABS) blends

where multiple grades of ABS were combined with the thermoplastic rubber (TPR) styrene ethylene butylene styrene (SEBS) in different weight ratios in the creation of a material system with tunable rigidity. Here, the intended application was dampeners (bumpers).

The shape memory properties of variants of the ABS-SEBS blends first developed by our group and presented in Siqueiros et al. (Siqueiros et al., 2016) was explored by Chávez et al. (Chávez et al., 2018) where it was found that shape memory values, namely shape fixation ratio (R_f) and shape recovery ratio (R_r) varied with the composition of SEBS content. Additionally, it was reported that these shape memory properties differed depending on the print raster pattern. In this prior work and additional studies pertaining to shape memory polymers performed by others (Alan Schoener et al., 2010; Lai and Lan, 2013a; Memarian et al., 2018), R_f and R_r are calculated as follows:

$$R_f(\%) = \frac{\varepsilon_u}{\varepsilon_m} \times 100\% \quad (1)$$

$$R_r(\%) = \frac{\varepsilon_m - \varepsilon_p}{\varepsilon_m} \times 100\% \quad (2)$$

where deformation is performed in a tensile testing machine and ε_u is the elongation of the specimen after the load is removed, ε_m is the maximum strain the specimen is subjected to (usually 100% elongation) and ε_p is the elongation of the specimen after recovery. In most cases involving thermoplastic shape memory polymers, recovery is achieved by heating the specimens. Overall shape memory effect can be assessed by the shape memory index (SMI) which is a combination of the two parameters calculated above and attained by the following equation (Chávez et al., 2018; Lai and Lan, 2013b):

$$SMI(\%) = (R_r \times R_f) \times 100\% \quad (3)$$

Though the study performed by Chávez et al. revealed noteworthy nuances related to the shape memory characteristics of the ABS-SEBS material system as used in AM processing, the blend itself was not designed with the intent of creating a shape memory material. The work presented here describes an initial materials characterization of a novel shape memory polymer system that is compatabile with FDM™-type AM platforms. Overall, the shape memory effect of polymeric materials are categorized by three classifications: 1) dual state, where the shape memory effect is driven by strong (covalent bonds holding the permanent shape, for example) and weak (chain entanglement holding the temporary shape, for example) crosslinks; 2) dual component, where the shape memory effect is driven by hard and soft phases that can be either on the molecular or micro scale; and 3) partial transition, where mixtures of two materials, one of which changes phase (solid to liquid for example) control the shape memory effect (Yang et al., 2014).

In this work, we chose to combine materials with different shape memory mechanisms in order to ascertain which type would contribure more to the overall shape mempry effect of resultant polymer blend. Polylactic acid (PLA), which posesses shape memory characteristics

driven by the dual state shape memory effect was combined with SEBS whichhas a shape memory effect driven by the dual component mechanism. The overall scope of this project entails the use of two elastomeric materials. These two different elastomeric materials were chosen because we also wished to explore the effects of miscbility on the overall shape memory effect. PLA and TPU would be expected to blend well together because their solubility parameters (δ) are similar with values of roughly 20 to 20.5 $MPa^{1/2}$ (Siemann, 1992; Wang et al., 2018). In contrast, SEBS has a solubility parameter of roughly 17 $MPa^{1/2}$ (Peng Wu et al., 2011) so it was expected that the result of combining SEBS with PLA would result in an imiscible blend. Additionally, the previous work presented in Chávez et al. revealed the ABS-SEBS blend to be an immiscible blend by way of scanning transmission electron microscopy (STEM), which also indicated that the varouis phases aligned with the print direction. The imiscibility was predictable as ABS has a solubility parameter ranging from 20 to 23 $MPa^{½}$ (Peng et al., 2010) and it was hypothesized that the alignment of the imisible phases had an effect on the shape memory parameters and their dependence on raster pattern. In the work presented here, it was thought that by creating miscible and imiscible blends the effect of phase alignment on the shape memory process could be deconvoluted from the well-known effect of print raster on mechanical properties, which has been documented heavily in literature (Perez et al., 2014; Torrado et al., 2015; Torrado and Roberson, 2016; Vega et al., 2011). The work presented here is the initial efforts in characterizing novel shape memory materials intended for use in FDM-Type additive manufacturing platforms. This project is still in the early phases and we will present data mainly pertaining to the PLA:SEBS blend system.

Experimental Procedure

PLA grade 4043D was combined with four weight percentages (5%, 10%, 25%, 50%) of styrene ethylene butadiene styrene with a maleic anhydride graft (SEBS-g-MA grade FG1901-GT, Kraton, Houston, TX, USA). Extrusion of a filament with a diameter of 2.85 +/- 0.05 mm was obtained using Collin twin screw extruder/compounder Model ZK 25T (Collin Lab and Pilot Solutions, Norcross, GA, USA).–Later, filaments were dried using VWR Forced air oven 3.65 (VWR International, PA, USA) at 80°C for 4 hours.

Tensile test specimens were obtained using Lulzbot TAZ 6 (Aelph Objects Inc., Loveland, CO, USA) following the ASTM Standard D638 in accordance with the Type IV specimen geometry. The tensile test specimens were printed in a longitudinal raster pattern with the print raster parallel to the direction of applied stress. The samples were printed with an infill of 100%. The impact specimens were also printed on Lulzbot systems, however a crosshatched raster pattern (alternating 45° layers in the XYZ direction) was used. The printing temperature of the blends increased as the weight percentage increased, therefore to improve bed adhesion Elmer's Glue Stick was used. Impact specimens were obtained using Lulzbot Taz 5 FlexyDually (Aelph Objects, Inc., Loveland, CO, USA) following ASTM Standard D256-10 in the XYZ direction with a 45° raster pattern and printed stress concentrator. The build orientation was chosen because it was demonstrated by Roberson et al. (Roberson, Torrado Perez, et al., 2015) that this orientation has the greatest resistance to impact. Printing parameters for the materials are listed in Table 1.

Table 1. Printing parameters

	PLA:SEBS			
Ratio	5:95	10:90	25:75	50:50
Printing Temperature	205°C	210°C	225°C	260°C
Bed Temperature	60°C	60°C	60°C	60°C
Nozzle Diameter	0.6 mm	0.6 mm	0.6 mm	0.6 mm
Interior Fill Percentage	100%	100%	100%	100%
Primary Layer Height	0.2 mm	0.2 mm	0.2 mm	0.2 mm
Printing Speed	30 mm/s	30 mm/s	30 mm/s	30 mm/s
Filament Diameter	2.85 mm	2.85 mm	2.85 mm	2.85 mm

Mechanical properties of the compounded material systems were obtained through a variety of testing methods. Dynamic mechanical analysis (DMA) was performed using PerkinElmer Model DMA 8000 (PerkinElmer, Waltham, MA, USA). The average dimensions of the specimens were the following, length of 40 mm, width of 8 mm and thickness of 2 mm. Dual cantilever mode was used for testing of the specimens. The temperature scan ranged from -40°C to 110°C at a rate of 5°C/min. Tensile testing of the printed specimens was performed using MTS Criterion C-44 (MTS Systems Corporation, Eden Prairie, MN, USA) and carried out at a constant strain rate of 10mm/min. Properties such as ultimate tensile strength (UTS) were obtained. Izod impact testing was performed using Tinus Olsen Model IT 504 (Tinus Olsen, Horsham, PA, USA) and impacted with a nominal weight of 1553.5 +/- 7.6 grams and latched pendulum potential energy of 7.44 Joules. Horizon software was used to determine the impact resistance, impact strength, and specimen break type.

Fracture surface analysis of spent impact test specimens was carried out through the use of a Hitachi SU-3500 (Hitachi America, Ltd, New York USA) scanning electron microscope. To reduce the effect of charging, the SEM was operated in variable pressure mode operating at 90 Pa and images were acquired through the use of a backscatter electron (BSE) detector or an ultra-variable detector (UVD). X-Ray diffraction was carried out through the use of a Bruker D8 Discover X-Ray Diffractometer (Bruker Scientific LLC, Billerica, MA, USA).

Results

Dynamic Mechanical Analysis (DMA) of the blend systems allowed for the determination of the glassy onset temperature as well as the max tan δ temperature. Our lab has found this data useful in the establishment of high temperature deformation and recovery temperatures for SMP materials. Illustrated in Figure 1 for PLA 4043D, if one were to deform a specimen at an elevated temperature, the glassy onset temperature could be used as the deformation temperature, while the original shape could be recovered by reheating the specimen to the max tan δ temperature. This figure is used as a reference/control for our material, where the deformation temperature is the temperature at which a material is deformed. While the recovery temperature is the temperature at which a material recovers to its full original shape. The DMA curves for the PLA:SEBS system are seen in Figure 2. The DMA results are numerically h illustrated in Table 2; where it can be seen for for 5% SEBS, 10% SEBS, 25% SEBS and 50% SEBS we obtained a tan δ of approximately 1. 70, 1.54, 1.10 and 0.60, respectively. We also noticed that the temperature stayed constant around 80 ° C for all four blends. From the figure three notable obserevations can be made: 1) the window between max tan δ and glassy onset decreases with an increase in SEBS content (especially apparent when comparing with the curve for PLA in Figure 1); 2) the storage modulus decreases with an increase in SEBS content; and 3) the max tan δ value decreases with an increase in SEBS content.

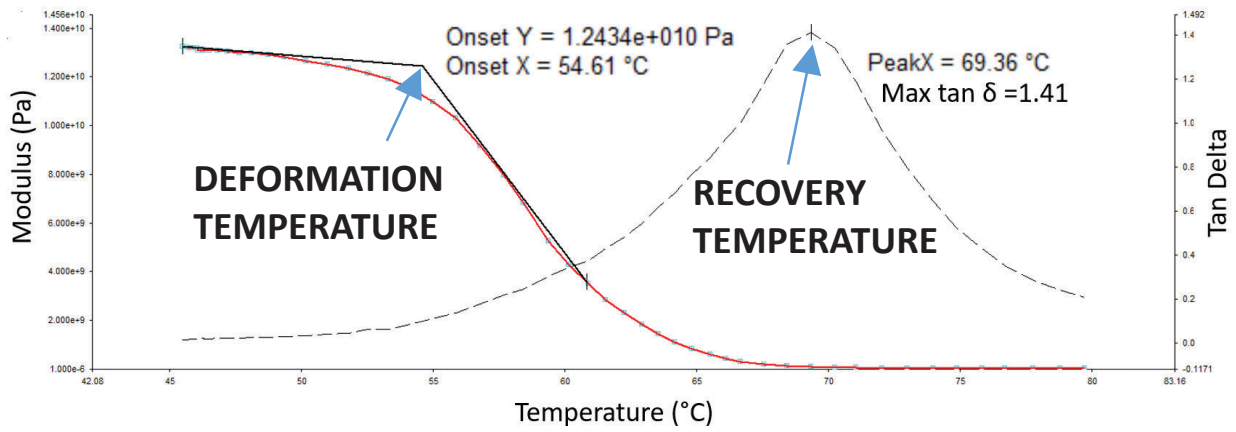

Figure 1. Utilization of DMA data to determine the critical temperatures for shape memory polymers.

Table 2. DMA Spectra Results.

Blends	*Tan Delta (Approx.)*	*Temperature (° C)*
PLA/SEBS 5%	**1.70**	**80° C**
PLA/SEBS 10%	**1.54**	**80° C**
PLA/SEBS 25%	**1.10**	**80° C**
PLA/SEBS 50%	**0.60**	**80° C**

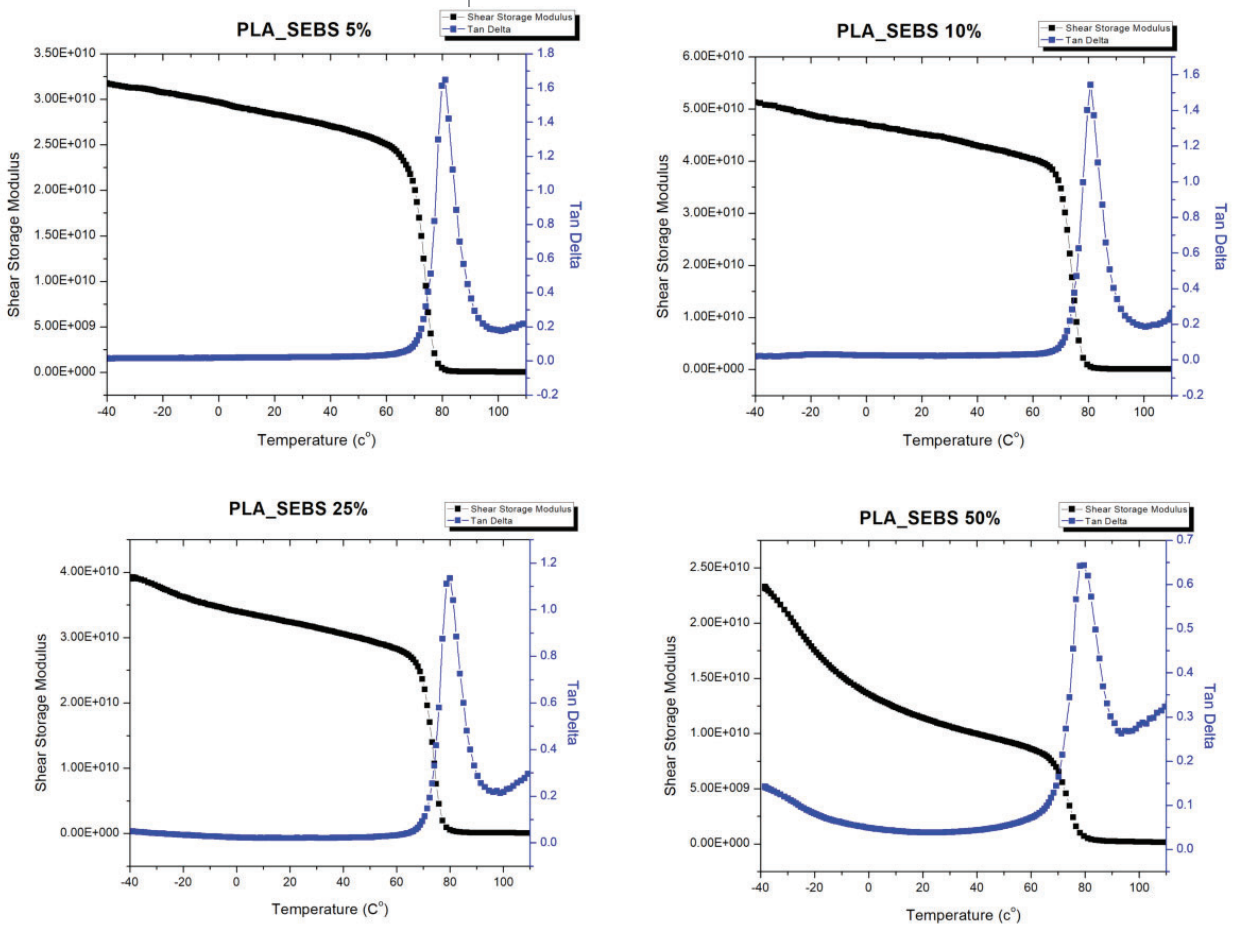

Figure 2. DMA Spectra for the PLA:SEBS blend system.

Impact testing of the PLA:SEBS material system revealed the 5% and 10% rubber content blends to be statistically the same in terms of impact properties, but an increase in impact strength of the material with an increase in rubber content was observed for the 25% and 50% rubber content blends. Table 3 is of the impact values while, for brevity, we have plotted the impact strength in Figure 3. It is notable that none of the test specimens tested here totally ruptured due to the Izod impact test. All specimens were "hinged" after impact. This could be due to the presence of rubber in the material. Examples of this are exhibited in Figure 4.

Table 3. Impact Test Values

% SEBS	Impact Strength, J/m^2		Impact Resistance, J/m		Break Energy, J		Sample size (n)
5%	4725.00	815.00	49.05	8.75	0.61	0.11	2
10%	4345.00	1145.00	45.15	11.75	0.57	0.15	2
25%	5853.33	3401.10	57.90	39.86	0.77	0.45	3
50%	19133.33	6451.01	201.33	67.61	2.53	0.84	3

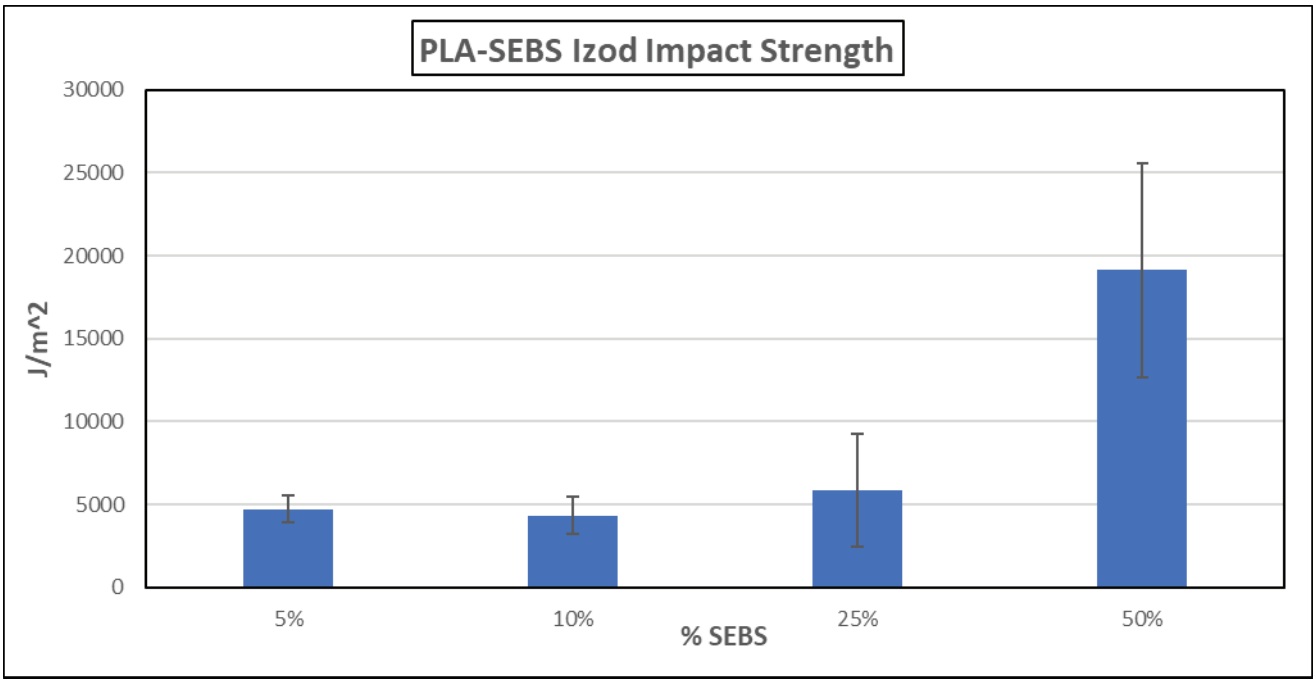

Figure 3. Impact strength of the PLA:SEBS material system studied here.

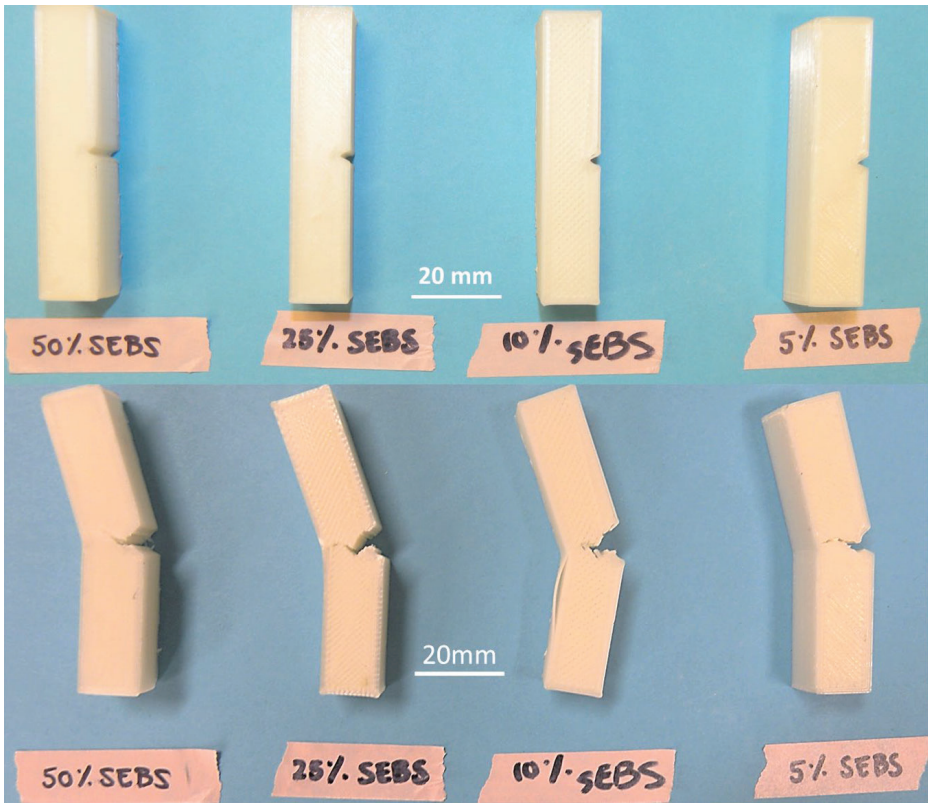

Figure 4. Examples of hinged failure.

SEM microanalysis of the fracture surfaces of representative specimens from the PLA:SEBS blend revealed that the fracture mode changes with an increase in SEBS content. All images were taken near the stress concentrator (V notch) of the specimens. Starting with Figure 5a the fracture surface morphology is that of brittle mode failure. The steps on the surface are opened up craze cracks indicative of brittle failure (Perez et al., 2014). The fracture surface in Figure 5b is of the PLA:SEBS 90:10 blend. The higher rubber content has increased the ductility of the material and there is a greater amount of plastic deformation that has been seen in the micrograph of the PLA:SEBS 5:95 blend in Figure 5a. Both Figures 5c and 5d exhibit a greater amount of plastic deformation indicative of brittle mode failure where the bottleneck features in Figure 3d indicate necking of the individual print rasters occurred due to the impact testing. Large fibrils are highlighted by arrows in Figures 5c and 5d, which are also indicative of ductile rupture.

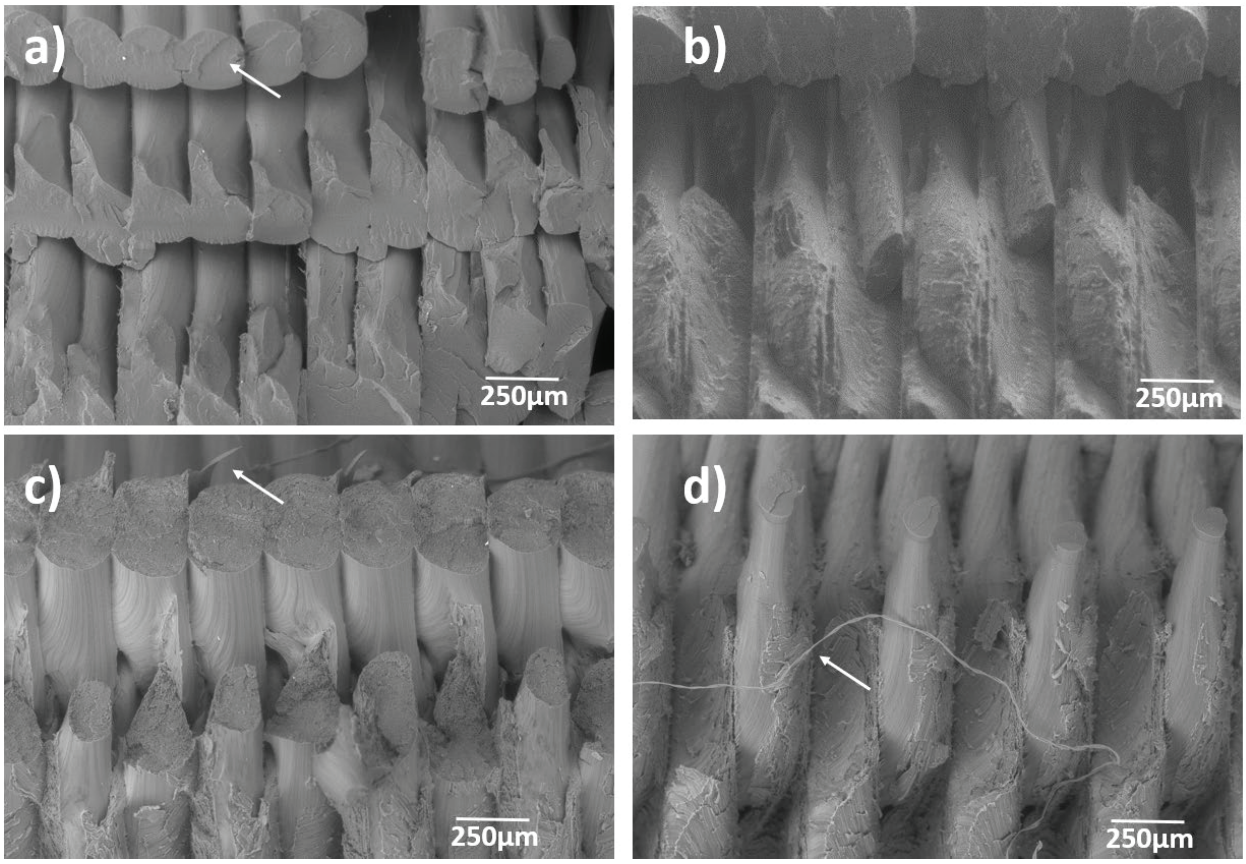

Figure 5. SEM Micrographs of Impact test specimens.

Analysis of the specimens via X-Ray diffraction revealed that all specimens of various PLA:SEBS compositions are amorphous in the as-printed state. The key indicator of this material property is the amorphous halo present spanning roughly 10 and 26 degrees on the 2θ scale. The halo is less prominent for the 5% rubber content blend. A noteworthy observation made in this study was that the blend systems containing 5%, 25% and 50% rubber exhibited crystallinity after DMA testing as indicated by the peaks. PLA alone is known to be heat-treatable to the point of inducing crystallinity (Rocha Gutierrez, 2016) so at this point, it is unclear as to why only the 5%, 25% and 50% rubber content blends are crystallized by the DMA testing. The XRD spectra is seen in Figure 6.

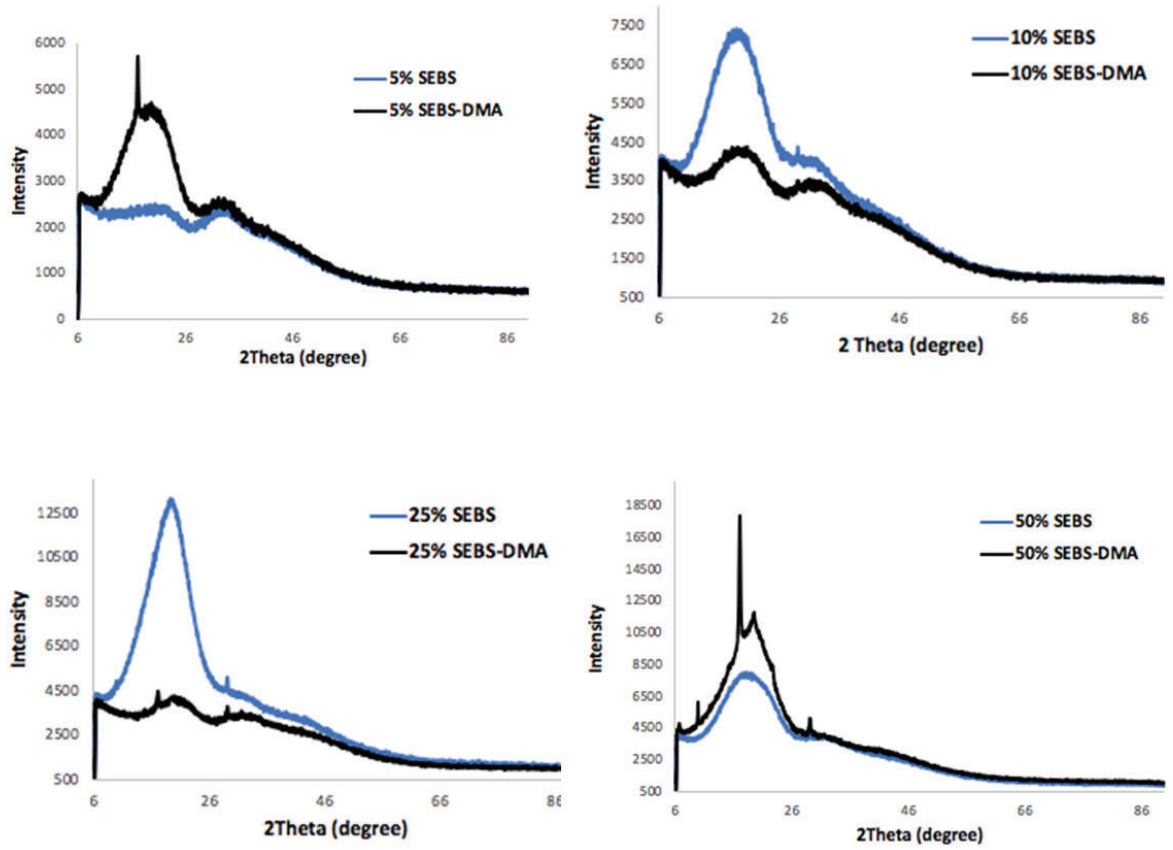

Figure 6. XRD Spectra for the PLA:SEBS blends.

Initial efforts at determining the shape memory properties of the PLA:SEBS material system are limited, however, our initial findings using tensile specimens with a composition of 25% SEBS demonstrated strong shape recovery ratios (R_r), and shape fixation ratios (R_f) as seen in Table 2. The specimen was elongated at room temperature to 100% elongation and then the load was released to record the ε_u value. The specimen was then heated at 80°C (the max tan δ temperature) in an oven for five minutes, removed, let to cool to room temperature, and then the ε_p value was recorded. The sequence of events is seen in Figure 7. Our testing revealed the PLA:SEBS blend at the 75:25 ratio to have R_f values of 88% and R_r values of 97%

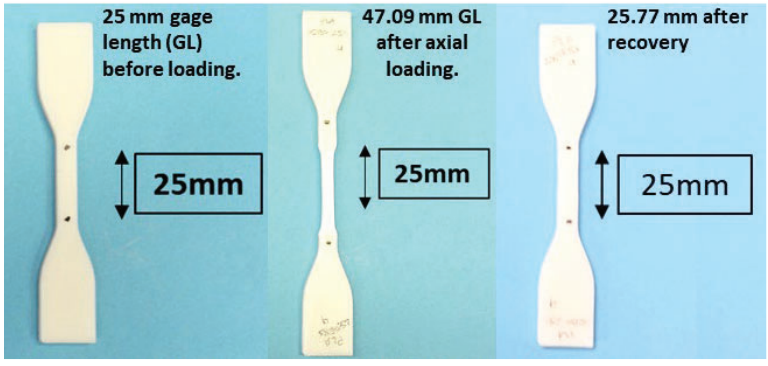

Figure 7. The shape memory testing process.

Conclusions

The combination of PLA with the thermoplastic rubber SEBS at different weight ratios yields a material system compatible with desktop-grade FDM™-type additive manufacturing platforms. Though, at this point in time data related to the shape memory characteristics is extremely limited, the blend of 75:25 PLA:SEBS yields a material that can be deformed at room temperature to a temporary shape and then recovered to nearly the original shape by heating at the max tan δ temperature of 80°C. Impact resistance of the PLA:SEBS system increases at loadings higher than 10% SEBS. The DMA testing process seems to induce crystallinity for some of the PLA:SEBS blends.

Future Work

Previous work carried out by our lab as presented by Chávez et al. (Chávez et al., 2018) serves as a template for future research activities. Pertinent future work includes assessing the effect of raster pattern on shape memory properties as characterization of the polymer phases present in the blends trough scanning transmission electron microscopy (STEM). Additionally, deformation at elevated and sub-zero temperatures will be performed as our prior work has shown that deformation temperature changes which shape memory parameter, R_f or R_r dominates the overall shape memory performance. We will also be comparing this results to a PLA with TPU blend that also yields printable material.

References

Alan Schoener, C., Bell Weyand, C., Murthy, R. and Ann Grunlan, M. (2010), "Shape memory polymers with silicon -containing segments", *Journal of Materials Chemistry*, Vol. 20 No. 9, pp. 1787–1793.

Chávez, F.A., Siqueiros, J.G., Carrete, I.A., Delgado, I.L., Ritter, G.W. and Roberson, D.A. (2018), "Characterisation of phases and deformation temperature for additively manufactured shape memory polymer components fabricated from rubberised acrylonitrile butadiene styrene", *Virtual and Physical Prototyping*, Vol. 0 No. 0, pp. 1–15.

Lai, S.-M. and Lan, Y.-C. (2013a), "Shape memory properties of melt-blended polylactic acid (PLA)/thermoplastic polyurethane (TPU) bio-based blends", *J Polym Res*, Vol. 20 No. 5, p. 140.

Lai, S.-M. and Lan, Y.-C. (2013b), "Shape memory properties of melt-blended polylactic acid (PLA)/thermoplastic polyurethane (TPU) bio-based blends", *J Polym Res*, Vol. 20 No. 5, p. 140.

Memarian, F., Fereidoon, A. and Ghorbanzadeh Ahangari, M. (2018), "Effect of acrylonitrile butadiene styrene on the shape memory, mechanical, and thermal properties of thermoplastic polyurethane", *Journal of Vinyl and Additive Technology*, Vol. 24, pp. E96–E104.

Peng, P., Shi, B., Jia, L. and Li, B. (2010), "Relationship between Hansen Solubility Parameters

of ABS and its Homopolymer Components of PAN, PB, and PS", *Journal of Macromolecular Science, Part B*, Vol. 49 No. 5, pp. 864–869.

Peng Wu, P., Shuhua Qi, S., Nailiang Liu, N., Kangqing Deng, K. and Haiying Nie, H. (2011), "Investigation of Thermodynamic Properties of SIS, SEBS, and Naphthenic Oil by Inverse Gas Chromatography", *Journal of Elastomers & Plastics*, SAGE PublicationsSage UK: London, England, Vol. 43 No. 4, pp. 369–386.

Perez, A.R.T., Roberson, D.A. and Wicker, R.B. (2014), "Fracture Surface Analysis of 3D-Printed Tensile Specimens of Novel ABS-Based Materials", *J Fail. Anal. and Preven.*, Vol. 14 No. 3, pp. 343–353.

Roberson, D., Shemelya, C.M., MacDonald, E. and Wicker, R. (2015), "Expanding the applicability of FDM-type technologies through materials development", *Rapid Prototyping Journal*, Vol. 21 No. 2, pp. 137–143.

Roberson, D.A., Torrado Perez, A.R., Shemelya, C.M., Rivera, A., MacDonald, E. and Wicker, R.B. (2015), "Comparison of stress concentrator fabrication for 3D printed polymeric izod impact test specimens", *Additive Manufacturing*, Vol. 7, pp. 1–11.

Rocha Gutierrez, C.R. (2016), *Improving the Engineering Properties of PLA for 3D Printing and Beyond*, The University of Texas at El Paso, United States – Texas, available at: https://search.proquest.com/docview/1803936514/abstract/593F598998924A60PQ/1.

Shemelya, C.M., Rivera, A., Perez, A.T., Rocha, C., Liang, M., Yu, X., Kief, C., et al. (2015), "Mechanical, Electromagnetic, and X-ray Shielding Characterization of a 3D Printable Tungsten–Polycarbonate Polymer Matrix Composite for Space-Based Applications", *Journal of Elec Materi*, Vol. 44 No. 8, pp. 2598–2607.

Siemann, U. (1992), "The solubility parameter of poly(dl-lactic acid)", *European Polymer Journal*, Vol. 28 No. 3, pp. 293–297.

Siqueiros, J.G., Schnittker, K. and Roberson, D.A. (2016), "ABS-maleated SEBS blend as a 3D printable material", *Virtual and Physical Prototyping*, Vol. 11 No. 2, pp. 123–131.

Torrado, A.R. and Roberson, D.A. (2016), "Failure Analysis and Anisotropy Evaluation of 3D-Printed Tensile Test Specimens of Different Geometries and Print Raster Patterns", *J Fail. Anal. and Preven.*, Vol. 16 No. 1, pp. 154–164.

Torrado, A.R., Shemelya, C.M., English, J.D., Lin, Y., Wicker, R.B. and Roberson, D.A. (2015), "Characterizing the effect of additives to ABS on the mechanical property anisotropy of specimens fabricated by material extrusion 3D printing", *Additive Manufacturing*, Vol. 6, pp. 16–29.

Vega, V., Clements, J., Lam, T., Abad, A., Fritz, B., Ula, N. and Es-Said, O.S. (2011), "The Effect of Layer Orientation on the Mechanical Properties and Microstructure of a Polymer", *J. of Materi Eng and Perform*, Vol. 20 No. 6, pp. 978–988.

Wang, C., Kou, B., Hang, Z., Zhao, X., Lu, T., Wu, Z. and Zhang, J.-P. (2018), "Pigment & Resin Technology Tunable shape recovery progress of thermoplastic polyurethane by solvents Article information:"Recent development in electrospun polymer fiber and their composites with shape memory property: a review" For Authors Tunable shape

recovery progress of thermoplastic polyurethane by solvents", *Pigment & Resin Technology*, Vol. 47 No. 1, pp. 47–54.

Yang, W.G., Lu, H., Huang, W.M., Qi, H.J., Wu, X.L. and Sun, K.Y. (2014), "Advanced Shape Memory Technology to Reshape Product Design, Manufacturing and Recycling", *Polymers*, Vol. 6 No. 8, pp. 2287–2308.